Polaronic transport properties in $La_{1-x}Sr_xFeO_3$ systems (0.05<or=x<or=0.3)

1995 J. Phys.: Condens. Matter 7 1215

(http://iopscience.iop.org/0953-8984/7/6/022)

J. Phys.: Condens. Matter 7 (1995) 1215–1227. Printed in the UK

Polaronic transport properties in $La_{1-x}Sr_xFeO_3$ systems ($0.05 \leqslant x \leqslant 0.3$)

W H Jung and E Iguchi†

Materials Science, Department of Mechanical Engineering and Materials Science, Faculty of Engineering, Yokohama National University, Tokiwadai, Hodogaya-Ku, Yokohama 240, Japan

Received 26 September 1994, in final form 21 November 1994

Abstract. Electrical transports in the $La_{1-x}Sr_xFeO_3$ system ($0.05 \leqslant x \leqslant 0.3$) was investigated as a function of temperature from 80 K to 350 K by dielectric properties, DC and AC conductivities. Two dielectric relaxation peaks appeared and their relative peak heights were closely related to the amount of Sr. The intensities of both these peaks were thermally activated. In every specimen, there was an Arrhenius relation between σT and T, the activation energy of which was nearly equal to the sum of the activation energy required for the dielectric relaxation and that for the thermal activation in the intensity of the relaxation peak. The frequency dependences of AC conductivities obeyed an equation of $\sigma(\omega) = A\omega^s$ and AC conductivities were independent of temperature below ~200 K at every applied frequency. These results were explained self-consistently with small polarons of ligand holes ($3d^5\underline{L}$) which were transformed from the states of O 2p weight to the mixed Fe 3d–O 2p states with an increase in the covalent character as the amount of Sr increases, as confirmed by the soft-x-ray spectroscopies and XPS-experiments.

1. Introduction

Controlled valence materials like $La_{1-x}Sr_xMO_3$ (where M is a first-row transition metal) show very interesting changes in their physical and chemical properties as a function of composition [1–4]. In particular, electrical transport properties are of great interest. It was generally assumed that replacement of La^{3+} by Sr^{2+} in these materials would lead to change in the 3d electron configuration, thereby providing a means to control the valence of the transition metal ions. It is likely that electrical transport properties in $La_{1-x}Sr_xMnO_3$ and $La_{1-x}Sr_xCoO_3$ are explained in terms of double exchange interactions between transition metal ions, as proposed by Zener [5–10]. In $La_{1-x}Sr_xFeO_3$, however, such interactions between Fe^{3+} and Fe^{4+} cannot be expected [6] and, alternatively, a thermally activated hopping process of small polarons between Fe ions appears to play an important role in transport properties [11–15].

According to the recent study on the soft-x-ray absorption spectroscopies by Abbate *et al* [16], however, the main component of the $LaFeO_3$ ground state is high-spin $3d^5$ which becomes $t_{2g}^3e_g^2$ in octahedral field. As La^{3+} is replaced by Sr^{2+}, the holes go to states of primary O 2p character and the main component of the ground state becomes $3d^5\underline{L}$ (where $\underline{L}$ denotes a ligand hole). For low Sr contents, these states are primarily made up of O 2p weight, while a transition to new states of mixed Fe 3d–O 2p character takes place as the amount of Sr increases. In addition, replacement of La^{3+} by Sr^{2+} in $La_{1-x}Sr_xFeO_3$ leads to an increase in the covalent character of the ground state. Though the covalent contribution

† Author to whom correspondence should be addressed.

0953-8984/95/061215+13$19.50

appears remarkably in the nature of ligand holes above $x \cong 0.5$ in soft-x-ray absorption spectroscopies, this contribution has a possibility of participating in the change of nature of ligand holes even at $x < 0.5$. The same characteristics of ligand holes in $La_{1-x}Sr_xFeO_3$ are reconfirmed also in XPS experiments by Chainani *et al* [17].

The results obtained by the soft-x-ray absorption and XPS, therefore, rekindle studies on electrical transports in $La_{1-x}Sr_xFeO_3$. If polaronic conductions take place virtually in this system as much of the literature suggests [6, 8–11], more direct evidence for hopping dynamics of polarons is required besides the experiments to date. As confirmed experimentally in our previous reports [18–20], dielectric measurements are very sensitive to a thermally activated hopping process of polarons because this process requires a dielectric relaxation. Besides our previous experiments, in fact, similar relaxations due to hopping processes of polarons are observed in other oxides like WO_3, Sm_2O_3–P_2O_5 glass and so on [21–23]. Dielectric measurements, therefore, have a high possibility of detecing directly the transition of ligand holes from O 2p weight to Fe 3d–O 2p mixed, even if other experimental methods like DC conductivity measurement are insensitive to this transition.

Considering these facts, it is of great significance to investigate transport properties in $La_{1-x}Sr_xFeO_3$. In our last report [24], we carried out an investigation on $LaFe_{1-x}Ti_xO_3$ and confirmed the polaronic conductions due to ligand holes, $3d\underline{L}$, and the compensation of holes by electrons introduced by replacements of Fe^{3+} with Ti^{4+}. In this report, we have measured dielectric properties, AC and DC conductivities of $La_{1-x}Sr_xFeO_3$ ($0.05 \leqslant x \leqslant 0.3$) in the temperature range of 80–350 K in order to investigate transport properties and will discuss the results in terms of small polarons of ligand holes the character of which is expected to change as a function of Sr composition.

2. Experimental procedure

The $La_{1-x}Sr_xFeO_3$ ceramic specimens ($x = 0.05$, 0.10, 0.20, 0.25 and 0.30) were prepared by the solid state synthesis technique. Powders of La_2O_3, Fe_2O_3 and $SrCO_3$ (Johnson Matthey, 5N grade) were used. The mixed powders were calcined in air at 1373 K for 24 h, then pressed into pellets and fired finally in air at 1623 K for 24 h. Specimens are numbered using terminology such as S-5, where the number denotes the amount of Sr in atomic ratio, here $La_{0.95}Sr_{0.05}FeO_3$. Powder x-ray measurements on the specimen, S-20, indicated the single phase of $La_{0.8}Sr_{0.2}FeO_3$ (an orthorhombic perovskite structure), which agrees with the data in JCPDS (code 35-1480).

Flat surfaces of specimens were coated with an In–Ga alloy in 7:3 ratio by a rubbing technique for an electrode in measurements of capacitances and conductances at low temperatures, but evaporated gold was used for measurements above 300 K. HP 4274A, 4275A and 4284A LCR meters were used for capacitance and conductance measurements, while a Keithley 619 resistance bridge, an Advantest TR 6871 digital multimeter and an Advantest R 6161 power supply were used for DC conductivity measurements by the four-probe method. A copper–constantan thermocouple precalibrated at 4.2, 77 and 273 K was used for the temperature measurements.

3. Experimental results

Figure 1 demonstrates Arrhenius plots of σT against $1/T$. Below $\sigma T \sim 10^{-5}$ K Ω^{-1} cm^{-1}, conductivities were hard to measure by the four-probe method. An increase in conductivities

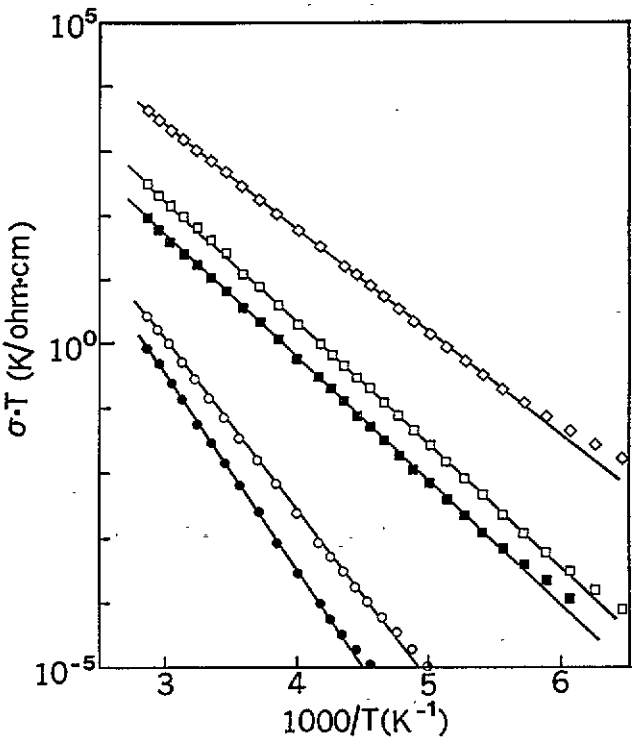

Figure 1. Arrhenius relations between σT and $1/T$ for $La_{1-x}Sr_xFeO_3$. Solid circles represent the results for specimen S-5 ($x = 0.05$); open circles, S-10 ($x = 0.10$); solid squares, $S-20$ ($x = 0.20$); open squares, S-25 ($x = 0.25$) and open diamonds, S-30 ($x = 0.30$).

with the amount of Sr is recognized obviously. In every specimen, there is a linear relation and the activation energies decrease as x increases, i.e., 0.53, 0.52, 0.42, 0.37 and 0.29 eV for specimens S-5, S-10, S-20, S-25 and S-30, respectively. At low temperatures, conductivities deviate from the linear relations. The conductivities increase rapidly as the amount of Sr increases from $x = 0.10$ to 0.20. One suspects, then, some correlation between such a non-linear increase in conductivities and a change of nature of carriers, i.e., the transfer from primary O 2p character to mixed Fe 3d–O 2p. Another increase in conductivities from $x = 0.25$ to 0.30 is observed again and this must be also due to a change of natures of carriers, but in this case, carriers in the specimen of S-30 contain a rather strong covalent composition in comparison with other specimens, as described in the introduction. $LaFeO_3$ is antiferromagnetic with the Néel temperature of ~750 K like as many other transition metal oxides. As x in $La_{1-x}Sr_xFeO_3$ increases, the Néel temperature decreases rapidly to ~400 K at $x \cong 0.30$ [25]. Even in the specimen S-30, however, the Néel temperature must be higher than the temperatures measured because there is no anomaly, in the plots of σT and $1/T$, due to the transition from the antiferromagnetic state to the paramagnetic one as shown in figure 1.

Figure 2 demonstrates the temperature dependence of the dielectric loss tangent, $\tan\delta$, of every specimen at the applied frequency, $f = 40$ kHz. When $x = 0.05$ and 0.10, i.e., specimens S-5 and S-10, one dielectric relaxation peak appears and this peak shifts to higher temperature and grows with increasing x. At $x = 0.20$ (i.e., S-20), this peak moves to a still higher temperature but decays. Instead of this weak peak, another strong

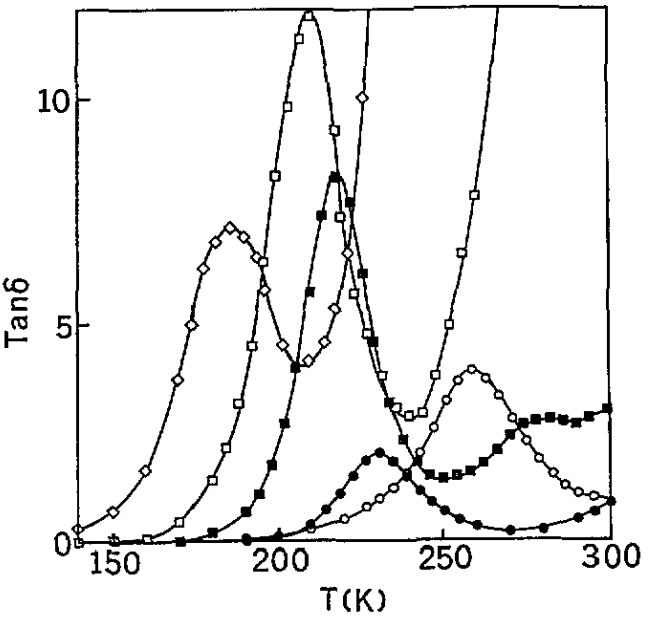

Figure 2. Temperature dependences of relaxation peaks in loss tangent, $\tan\delta$, at the applied frequency, $f = 40$ kHz. Solid circles represent the results for specimen S-5 ($x = 0.05$); open circles, S-10 ($x = 0.10$); solid squares, S-20 ($x = 0.20$); open squares, S-25 ($x = 0.25$) and open diamonds, S-30 ($x = 0.30$).

dielectric relaxation peak appears at a lower temperature. The latter shifts slightly to lower temperature and considerably grows as x changes from 0.20 to 0.25. However, it decays and becomes broad remarkably at $x = 0.30$. The appearance of two peaks in the specimen S-20 suggests that both the peaks belong to the same family and their relative intensities depend upon the environment variation caused by the change in the proportion of Sr ions present.

A Debye type dielectric relaxation involves the following relation for the loss tangent,

$$2\pi f \tau_0 \exp\left(\frac{Q}{k_B T_m}\right) = 1 \tag{1}$$

where Q denotes the activation energy required for the relaxation, k_B is Boltzmann's constant, f is the applied frequency, τ_0 represents the pre-exponential factor of the relaxation time and T_m is the temperature where the loss tangent is maximum. In Arrhenius plots of f against $1/T_m$ for the loss tangent, as shown in figure 3(a), one has good straight lines with activation energies of $Q = 0.49$ eV for the specimen S-5, 0.48 eV for S-10, 0.41 eV for the strong peak in S-20, 0.33 eV for S-25 and 0.23 eV for S-30. These energies are generally somewhat smaller than those obtained in figure 1. Denote the maximum value of $\tan\delta$ at T_m as $(\tan\delta)_{max}$, then the Debye's theory predicts that $(\tan\delta)_{max} \propto 1/T_m$. Arrhenius relations between $(\tan\delta)_{max}T_m$ and $1/T_m$, plotted in figure 3(b), however, imply that $(\tan\delta)_{max}$ increases as T_m increases. The good straight lines in figure 3(b) have activation energies 0.02–0.04 eV. The results for the small peak in the specimen S-20 are omitted for figure 3(a) and (b) because the contribution of this relaxation to dielectric properties and transport properties must be small compared with the strong relaxation, but the activation energy, Q, is found to be ~0.32 eV.

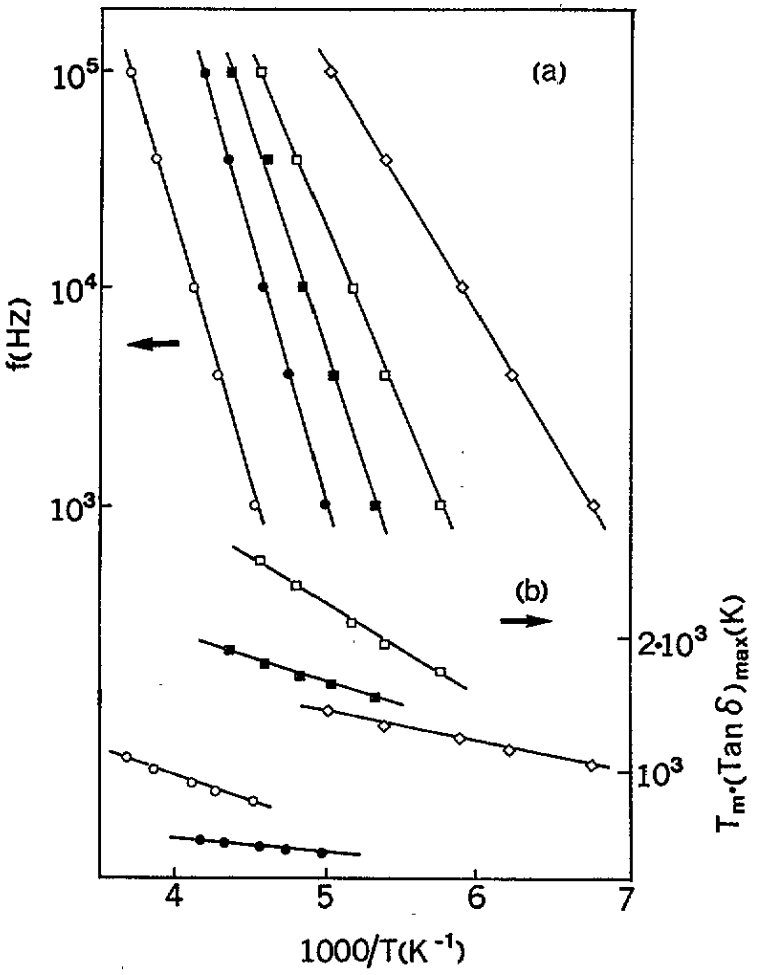

Figure 3. (a) Arrhenius relations between f and $1/T_m$, and (b) those between $T_m(\tan\delta)_{max}$ and $1/T_m$, where T_m is the temperature where the loss tangent is maximum, i.e., $(\tan\delta)_{max}$, and f is the applied frequency. Solid circles represent the results for specimen S-5 ($x = 0.05$); open circles, S-10 ($x = 0.10$); solid squares, S-20 ($x = 0.20$); open squares, S-25 ($x = 0.25$) and open diamonds, S-30 ($x = 0.30$).

The conductance measurements yield the real part of AC conductivities. Figure 4 demonstrates the Arrhenius relations between the AC conductivity, $\sigma(\omega)$, and temperature, T, for the specimen S-10 with the result for DC conductivities. At temperatures below ~200 K, $\sigma(\omega)$ is independent of temperature at every applied frequency. Other specimens show similar behaviours. The frequency dependence of AC conductivities, $\sigma(\omega) \propto \omega^s$, is confirmed in every specimen, where s is a temperature-dependent quantity. The values of β ($= 1 - s$) determined by least-mean-square analyses are plotted as a function of temperature at 10 K increments for specimens S-5 and S-25 in figure 5. In $LaFe_{1-x}Ti_xO_3$ [24], there are three temperature ranges, i.e., the low-temperature range where $\beta \cong 0$, the intermediate-range in which there exists a linear relationship between β and T, and the high-temperature range where β deviates from the linear relation and increases rather rapidly with increasing temperature. The specimens S-5 and S-10 exhibit behaviours quite similar

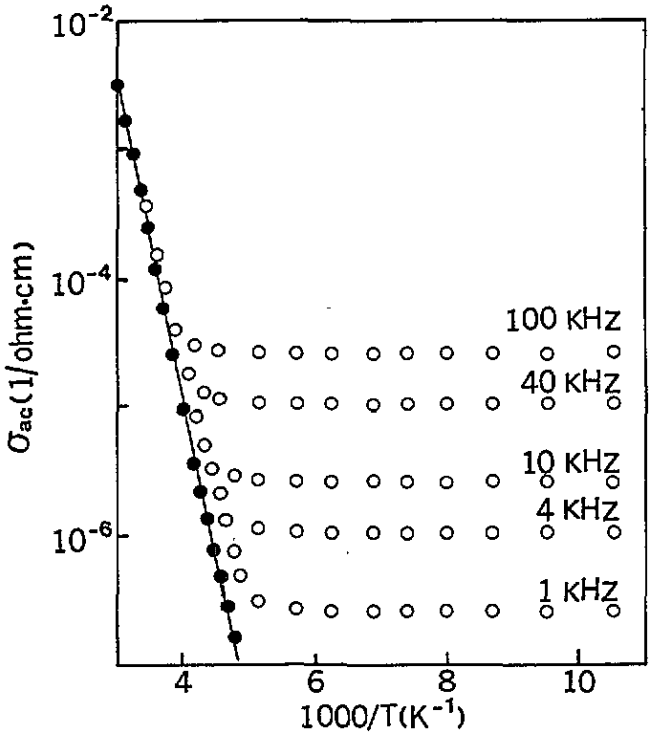

Figure 4. Arrhenius relations between AC conductivity, $\sigma(\omega)$, and $1/T$ at applied frequencies, f = 1, 4, 10, 40 and 100 kHz, (open circles), with the results for DC conductivities (solid circles) for the specimen S-10.

to $LaFe_{1-x}Ti_xO_3$, as shown in figure 5, while the intermediate ranges are not recognized in other specimens, i.e., S-20, S-25 and S-30. Though Pollak finds a frequency-dependent conductivity of the form [26]

$$\sigma(\omega) = A\omega\{\ln(\Omega_0/\omega)\}^4 \tag{2}$$

and Pollak and Geballe [27] have graphically shown that equation (2) is practically indistinguishable from a plot of $A'\omega^{0.8}$, this theoretical expression cannot account for the result in figure 5 because s changes as a function of T.

4. Discussion

4.1. Dielectric relaxations

As shown in figure 2, there are two dielectric relaxation peaks in the $La_{1-x}Sr_xFeO_3$ system: the one which mainly appears at low Sr contents is rather small and another one which is observed at x = 0.20–0.30 is rather strong. The small peak decays and, instead, the strong peak grows as the amount of Sr increases from x = 0.10 to 0.25, that is, the nature of the active dipoles responsible for the dielectric relaxations changes as a function of the amount of Sr. This feature corresponds well to the transition of ligand holes, $3d\underline{L}$, from O 2p weight to Fe 3d–O 2p mixed state observed in soft-x-ray spectroscopies [16].

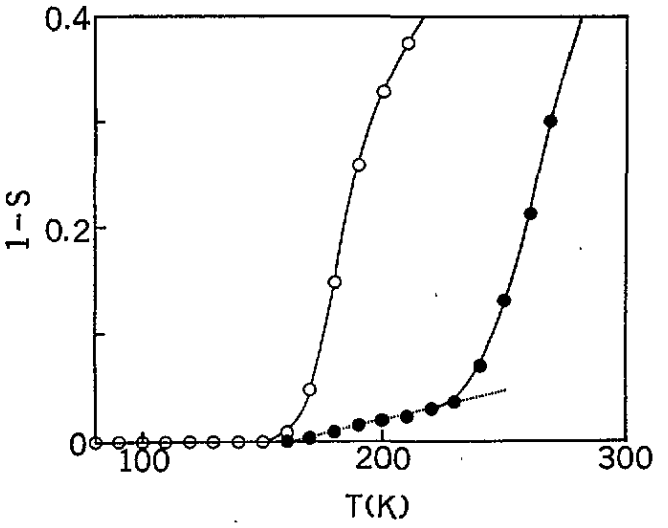

Figure 5. Plots of $(1 - s) = \beta$ as a function of temperature for the specimens S-5 (solid circles) and S-25 (open circles), where s is a temperature-dependent quantity in the relation of $\sigma(\omega) \propto \omega^s$. The broken line in the result for S-5 represents the linear part in which β is proportional to T.

This means that both of the relaxations observed belong to the same family as suggested before. The characteristics of the small peak reported in the previous section are quite similar to the dielectric relaxations observed in $LaFe_{1-x}Ti_xO_3$ [24]. The same sort of active dipole moment must be responsible for both the relaxations in $LaFe_{1-x}Ti_xO_3$ and those in $La_{1-x}Sr_xFeO_3$ at low Sr concentrations ($x \leqslant 0.10$).

In the case of ligand holes of O 2p weight at low Sr contents, their positions are rather close to oxygen ions and, then, the primitive distance of their hops must be the spacing between oxygen ions, i.e., $\sim \sqrt{2}a/2$, where a is the mean lattice constant. When ligand holes are in Fe 3d–O 2p mixed states at high Sr contents, they remove their positions towards Fe ions and, consequently, the hopping distance is expected to be the spacing between Fe ions, i.e., $\sim \sqrt{2}a$. According to the Debye theory, the loss tangent, $\tan\delta$, is proportional to the square of the hopping distance. Then, $(\tan\delta)_{max}$ due to Fe 3d–O 2p mixed ligand holes is roughly four times as large in values as that of O 2p ligand holes. This speculation accounts for the relative intensities of the two absorption peaks in figure 2. However, the ratio for the specimen S-30 to S-10 is approximately two. This is due to the characteristics of the sample S-30 which exhibits quite different behaviours from the others because of a rather strong covalent contribution involved in this specimen, which will be described later.

The backgrounds in the specimens of S-25 and S-30 rise at high temperatures as shown in figure 2. If the experiments could be carried out in the temperature range above room temperature, other specimens with low contents of Sr would show similar tendencies, as reported in our previous paper on α-$Li_xMn_3O_4$ [20]. Increases in polarizabilities induced by the misfit in ionic radii between La^{3+} and Sr^{2+} mainly enhance the dielectric constant as indicated by the Clausius–Mossotti relation [28] and, consequently, it is likely that ionic displacements associated with increased polarizabilities, at high temperatures, lead to the steep rises of backgrounds in the dielectric loss tangent which is proportional to the dielectric constant.

As described in the introduction, electrical transport due to a hopping process of small

polarons has been proposed for $LaFeO_3$ and $La_{1-x}Sr_xFeO_3$ [12–15]. If both of the dielectric relaxations observed in this text are of this mechanism, the activation energy Q in equation (1) should be $(W_h + W_d/2)$, where W_h denotes the hopping energy of a polaron and W_d is the disordered energy [18–20, 29]. In most cases of dielectric relaxations, a single relaxation time does not describe the relaxation process: rather, a distribution of relaxation times is required. The theoretical description of physical models exhibiting a distribution of relaxation times is often very complex. It is sufficient, however, to quote the results of a simple model [30, 31] in which the barrier heights involved for the polaron hopping are equally distributed between W_h and $(W_h + W_d)$. This model is also employed here.

Holstein [32] proposed the non-adiabatic expression

$$\tau_0^{-1} = \pi^{1/2} J^2 / 2\hbar (W_h k_B T)^{1/2}$$

where J is the transfer integral. Using this expression in conjunction with equation (1), the plots of $\log f(T_m)^{1/2}$ against $1/T_m$ provide values for J. Least-mean-square analyses yield J = 0.54, 0.11, 0.11, 0.02 and 0.002 eV for the specimens S-5, S-10, S-20, S-25 and S-30, respectively. These values except S-30 are not subject to the non-adiabatic condition [32, 33], i.e., $J < (W_h k_B T/\pi)^{1/4} (\hbar\omega_{LO})^{1/2}$, where ω_{LO} is the angular frequency of the longitudinal optical mode at the zero wave vector. Though the experimental value for ω_{LO} of $LaFeO_3$ is not yet available, optical phonon frequencies for similar materials lie in the range $\omega_{LO} = 10^{13}$–10^{14} s^{-1} [34, 35]. Then it looks reasonable to exclude non-adiabatic cases and small polarons of ligand holes must be the most realistic candidates for both dielectric relaxations.

Equation (1) yields jump frequencies $\nu_0 = \tau_0^{-1}$, 1.3×10^{16}, 4.8×10^{14}, 6.4×10^{14}, 2.5×10^{13} and 3.7×10^{11} s^{-1} for S-5, S-10, S-20, S-25 and S-30, respectively, which exceed the expected optical phonon frequency except S-30. Consequently, the dielectric relaxations observed are likely to be associated with motions of charge carriers, i.e., small polarons of ligand holes. The anomaly for S-30 will be discussed later.

As shown in figure 3(b), $(\tan\delta)_{max}$ increases with applied frequency. The Debye theory based upon a constant number of oscillators cannot explain this phenomenon because $(\tan\delta)_{max}$ is proportional to the number of dipoles responsible for the relaxation, and alternatively a thermal activation of the number of active dipoles is required [18–20, 30]. At low temperatures, small polarons of ligand holes are bound to some imperfections such as Sr^{2+} substituted for La^{3+} and the hopping of ligand holes with the activation energy of $(W_h + W_d/2)$ takes place as the temperature rises (i.e., free polarons). Then, the density of free polarons at temperature, T, is given by $n_0 \exp(-W_o/2k_B T)$ [18–20], where n_0 is the number of ligand holes per unit volume and W_o represents the potential difference between a polaron bound to a trap and a free small polaron. The activation energies obtained in figure 3(b), then, correspond to $W_o/2$.

4.2. DC conductivities

The dielectric behaviours suggest hopping motions of small polarons of ligand holes in $La_{1-x}Sr_xFeO_3$. If the electrical conduction is of this mechanism, the temperature dependence of the DC conductivity predicted by the polaron theories [29, 32, 36] is of the form

$$\sigma = T^{-1} e n_0 \exp\left(-\frac{W_h + W_d/2 + W_o/2}{k_B T}\right) \tag{3}$$

where e is the electronic charge. Good fits are obtained in Arrhenius plots of σT against $1/T$ in figure 1. This result contains several aspects. First, the energies obtained in figure 1 are nearly equal to the sums of $(W_h + W_d/2)$ obtained in figure 3(a) and $W_o/2$ in figure 3(b), as suggested in equation (3). Though the specimen S-20 contains two relaxations as demonstrated in figure 2, we have omitted the small peak for the reason described before. Thus, the relative correlation of the energies estimated separately by different means is explained self-consistently in terms of a hopping process of small polarons of ligand holes. Our experiments cannot separate $(W_h + W_d/2)$ into individual terms but $W_d/2$ is much smaller than W_h. In practice, it is less than the experimental error in the determination of W_h [30]. This will be confirmed in the next section. Second, the conductivity increases with increasing amount of Sr. This indicates an increase in the density of mobile carriers as a function of x. Though there is another possibility that a change in mobility with the material composition increases the conductivity, the relative relation of the conductivity and the Sr content seems to suggest a minor contribution of the mobility effect. Jonker obtained similar behaviours in the resistivity measurements at room temperature [37], but, in the present text, the conductivities increase rapidly when the amount of Sr exceeds $x = 0.20$. It should be emphasized that the rapid increase in conductivities is associated with the appearance of the strong dielectric relaxation as shown in figure 2. This correlation indicates that the nature of majority carriers responsible for the electrical transport changes when x exceeds beyond 0.20, although the activation energies required for the dielectric relaxations and electrical conductions change smoothly, never drastically.

The speculations discussed in the previous and the present sections (4.1 and 4.2) in conjunction with the analyses by Abbate *et al* on their soft-x-ray spectroscopies [16] lead to the conclusion that the dielectric relaxation at low Sr contents can be ascribed to the ligand holes of O 2p weight and another relaxation dominant at $x = 0.20$–0.30 is correlated with ligand holes of mixed Fe 3d–O 2p. These ligand holes are in small-polaron states and their hopping processes dominate the electrical transports in $La_{1-x}Sr_xFeO_3$. Dielectric relaxations, AC and DC conductivities observed at low Sr contents (S-5 and S-10) have general features in common with those in $LaFe_{1-x}Ti_xO_3$ which contains small numbers of ligand holes [24]. This fact, then, implies that small polarons of ligand holes of O 2p weight are the majority carriers responsible for transport properties in $LaFe_{1-x}Ti_xO_3$ and $La_{1-x}Sr_xFeO_3$ ($x \leqslant 0.10$).

The specimen S-30 exhibits somewhat anomalous behaviours in the intensity of the relaxation peak and the relaxation time. In addition, DC conductivities increase remarkably when x changes from 0.25 to 0.30, as described before. Such anomalies must be loosely attributed to the covalent contribution involved in the ground state. Abbate *et al* demonstrate increased covalency with increasing x, which is remarkable over $x = 0.50$ [16]. The present result, however, suggests that the covalent effects have some influence upon the nature of ligand holes, even at $x = 0.30$.

4.3. AC conductivities

The frequency dependence of the AC conductivity, $\sigma(\omega)$, is written as

$$\sigma(\omega) = \sigma - \sigma_{DC} = A\omega^s \tag{4}$$

where σ is the real part of the complex conductivity and A is a complex constant term. At low temperatures, DC conductivities are, in general, negligibly small compared with AC conductivities and then $\sigma(\omega) = \sigma \propto \omega^s$. In many materials [38–43], in fact, there exists an extended frequency range for which $\sigma(\omega) \propto \omega^s$ with $1 \geqslant s > 0.5$. In $LaFe_{1-x}Ti_xO_3$, as

described before, there are three temperature ranges in the plot of $\beta = 1 - s$ against T; the low-temperature range where $\beta \cong 0$, the intermediate range in which impurity conductions of small polarons occur and the high-temperature ranges [24].

As for the intermediate range, our previous report [24] adapted Pike's theory [44] to the DC impurity conduction proposed by Mott [45] and obtained the ω^s law in the temperature range in which Pike's assumption, $\beta = 6k_BT/W_m$, is applicable, where W_m is the ground state energy of a ligand hole localized state. Specimens S-5 and S-10 contain the intermediate ranges as well as $LaFe_{1-x}Ti_xO_3$ (see figure 5) and this is expected because the majority carriers in S-5 and S-10 are the small polarons with the same characteristics, O 2p weight, as those in $LaFe_{1-x}Ti_xO_3$. The ground state energy, W_m, introduced in Pike's theory represents the energy difference between the ground state of the potential well and the 'ionized' state. In the intermediate range, most of the ligand holes are bound to traps like Sr^{2+} substituted for La^{3+}. The potential energy of ligand holes in this state is W_m. As the temperature rises, ligand holes start to dissociate from traps and become free polarons. The potential energy of free polarons is the polaron binding energy, W_p, which is generally approximated by $2W_h$ [29], and the potential difference between a small polaron bound to a trap and a free polaron is W_o, as defined before. Then one obtains the relation, $W_m \cong (2W_h + W_o)$. The plots of β and T yield W_m = 1.06 eV and 1.01 eV for S-5 and S-10, while $(2W_h + W_o)$ = 1.03 eV and 1.01 eV for S-5 and S-10, respectively. The agreements are good, within experimental errors, as well as the results in $LaFe_{1-x}Ti_xO_3$ [24].

In the specimens S-20, S-25 and S-30, however, a direct transition from the low-temperature range to the high-temperature one, not through the intermediate range, takes place as shown in figure 5. In high-temperature ranges observed in all specimens, β becomes great rapidly. This is, as Pike indicated [44], due to the fact that small polarons can hop over large energy barriers at high temperatures. The reasons why the intermediate range does not appear for high Sr contents (S-20–S-30) are still unknown. One possibility is that the large overlapping of wave functions of ligand holes results in a decrease in the hopping energy and, consequently, small polarons of ligand holes can start hopping even at low temperatures.

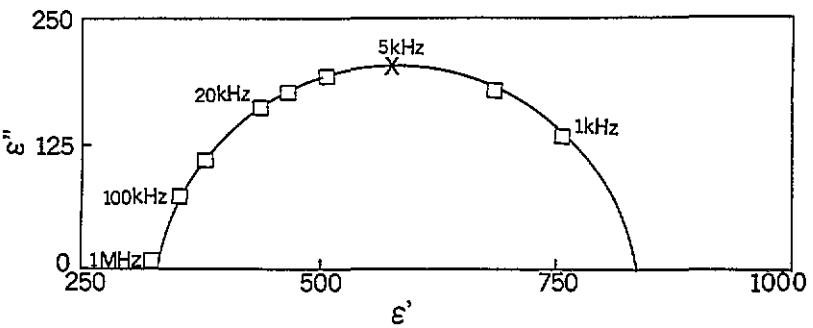

Figure 6. A Cole–Cole circular arc at $T = 220$ K for the specimen of S-5. The solid curve is the arc obtained by the least-mean-square analysis and the cross represents the maximum of the arc with $\omega_0 \cong 2\pi \times 5$ kHz in this case.

In every specimen in systems of both $LaFe_{1-x}Ti_xO_3$ and $La_{1-x}Sr_xFeO_3$, AC conductivities are independent of temperature in the low-temperature range where $s \cong 1$ (compare figure 4 with figure 5). Pollak and Pike investigated the AC conductivity due to

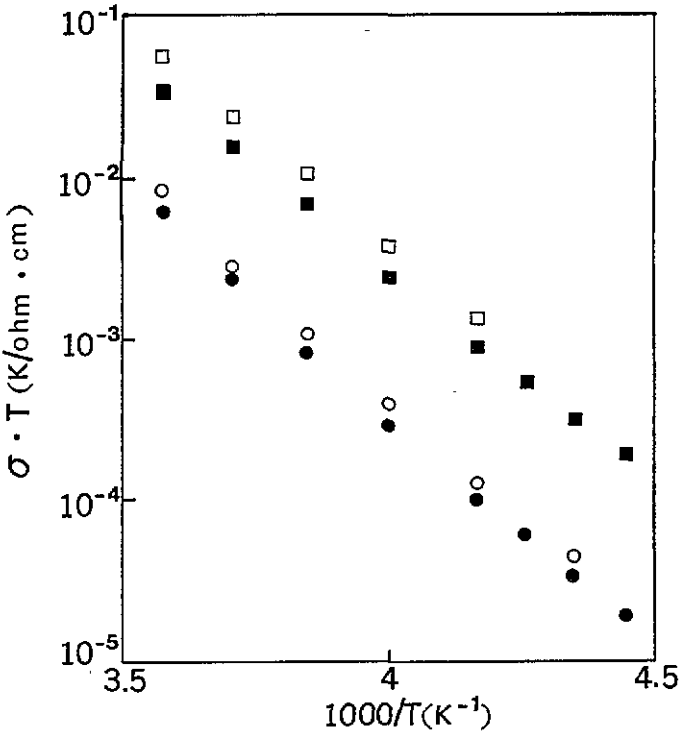

Figure 7. A comparison between the conductivities estimated from Cole–Cole plots and DC conductivities for the specimens S-5 and S-10 as a function of temperature. The open circles and squares represent the conductivities estimated from Cole–Cole plots for S-5 and S-10, respectively, while solid circles and squares are DC conductivities.

electronic quasiparticles which are relatively free to occupy either of two (or possibly more) non-degenerate sites by tunnelling between them through a thin barrier and obtained the theoretical expression for the AC conductivity [46]

$$\sigma(\omega) = \tfrac{1}{6}\pi\omega e^2 r_0^2 N k_B T \frac{\tanh(\overline{\Delta}/2k_B T)}{\overline{\Delta E}} \tag{5}$$

where N is the concentration of ligand holes which can hop and r_0 is the mean spacing between holes in the case of $La_{1-x}Sr_xFeO_3$. Pollak and Pike treated the AC conductivity in glasses but their theory is applicable in crystals. In equation (5), $\overline{\Delta}$ represents the upper limit in the distribution of the potential difference of non-degenerate sites, which is abbreviated as W_d in this text, and $\overline{E}$ denotes the maximum potential barrier which must be approximated reasonably by W_h in crystals. In glasses, $\overline{\Delta}$ has a magnitude detectable in experiments, while W_d is, in general, very small in crystals, less than experimental errors in the determination of W_h, as described before. Then,

$$\frac{\tanh(W_d/2k_B T)}{W_d W_h} \cong \frac{1}{k_B T W_h} \tag{6}$$

and, consequently,

$$\sigma(\omega) \cong \pi\omega e^2 r_0^2 N/6W_h. \tag{7}$$

The AC conductivity is, therefore, independent of temperature and an ω^1 law holds, as shown in figures 4 and 5, at low temperatures where tunnelling of holes through barriers takes place.

There is further evidence for a hopping process of small polarons in this system. If a dielectric relaxation process is of this mechanism, the characteristic frequency at the maximum of the Cole–Cole circular arc, ω_0, is the lower limit of the DC hop frequencies which is related to R and C_2 as follows [47]

$$\omega_0 R C_2 = 1 \tag{8}$$

where $C_2 = (\epsilon_0 - \epsilon_\infty)\varepsilon_0$, ϵ_0, ϵ_∞ and ε_0 being the static dielectric constant, the optical dielectric constant and the permittivity of free space, and R is the resistance. In the specimens investigated here, Cole–Cole plots extended generally to frequencies lower than the lower limit of our apparatus and the maxima in circular arcs were hard to obtain. However, for the specimens doped with low contents of Sr, S-5 and S-10, it was possible to plot the arcs at intermediate temperatures, as shown in figure 6 where the solid line is the circular arc calculated by the least-mean-square analysis, using the experimental plots (open squares), and the cross represents the maximum of the arc. Equation (8) means that the characteristic frequencies, ω_0, estimated from the maxima of the circular arcs provide conductivities. Figure 7 plots the conductivities obtained in this way which are compared with the DC conductivities. There are good agreements, although the conductivities estimated from Cole–Cole plots are slightly large in value compared with the DC conductivities. This result is consistent with the conclusion of the conduction being due to a hopping process of small polarons in $La_{1-x}Sr_xFeO_3$ as described before.

Acknowledgments

The authors are very grateful to N Kubota, K J Lee and N Nakamura for assistance in this project and useful discussion.

References

[1] Goodenough J B 1963 *Magnetism and the Chemical Bond* (New York: Wiley) ch 1
[2] Robin M B and Day P 1967 *Adv. Inorg. Chem. Radiochem* **10** 247
[3] Goodenough J B 1971 *Progress in Solid State Chemistry* vol 5, ed H Reiss (Oxford: Pergamon) p 145
[4] Rao C N and Gopalakrishnan J 1986 *New Diffractions in Solid State Chemistry* (Cambridge: Cambridge University Press) ch 1
[5] Zener C 1951 *Phys. Rev.* **82** 403
[6] Jonker G H 1956 *Physica* **22** 707
[7] Watanabe H 1957 *J. Phys. Soc. Japan* **12** 515
[8] Matsumoto G 1970 *J. Phys. Soc. Japan* **29** 615
[9] Tanaka T, Umehara M, Tamura S, Tsukioka M and Ehara S 1982 *J. Phys. Soc. Japan* **51** 1236
[10] Hasimoto T, Ishizuka N, Mizutani N and Kato M 1988 *J. Mater Sci.* **23** 1102
[11] Mizusaki J, Sasamoto T, Cannon W R and Bowen H K 1982 *J. Am. Ceram. Soc.* **65** 363
[12] Rao C N, Parkash O M and Ganguly P 1975 *J. Solid State Chem.* **15** 186
[13] Geller S and Wood E A 1956 *Acta Crystallogr.* **9** 563
[14] Mizusaki J, Sasamoto T, Cannon W R and Bowen H K 1983 *J. Am. Ceram. Soc.* **66** 247
[15] Koehler W C and Wollan E O 1957 *J. Phys. Chem. Solids* **2** 100
[16] Abbate M, de Groot F M F, Fuggle J C, Fujimori A, Strebel O, Lopez F, Domke M, Kaindl G, Sawatzky G A, Takano M, Takeda Y, Eisaki E and Uchida S 1992 *Phys. Rev.* B **46** 4511
[17] Chainani A, Mathew M and Sarma D D 1993 *Phys. Rev.* B **48** 14818

[18] Iguchi E, Kubota N, Nakamori T, Yamamoto N and Lee K J 1991 *Phys. Rev.* B **43** 8646
[19] Iguchi E and Akashi K 1992 *J. Phys. Soc. Japan* **61** 3385
[20] Lee K J, Iguchi A and Iguchi E 1993 *J. Phys. Chem. Solids* **54** 975
[21] Gehlig R and Salje E 1983 *Phil. Mag.* B **47** 229
[22] Mansingh A, Reyers J M and Sayer M 1972 *J. Non-Cryst. Solids* **7** 12
[23] Sidek A A, Collier I T, Hampton R N, Saunders G A and Bridge B 1989 *Phil. Mag.* B **59** 221
[24] Iguchi E and Jung W H 1994 *J. Phys. Soc. Japan.* **63** 3078
[25] Shimony U and Knudsen J M 1966 *Phys. Rev.* **144** 361
[26] Pollak M 1971 *Phil. Mag.* **23** 519
[27] Pollak M and Geballe T H 1961 *Phys. Rev.* **122** 1742
[28] Kittel C 1971 *Introduction to Solid State Physics* 4th edn (New York: Wiley) p 459
[29] Austin I G and Mott N F 1969 *Adv. Phys.* **18** 41
[30] Dominik L A K and MacCrone R K 1967 *Phys. Rev.* **163** 757
[31] Fröhlich H 1958 *Theory of Dielectrics* (Oxford: Clarendon) p 90
[32] Holstein T 1959 *Ann. Phys., NY* **8** 343
[33] Emin D 1971 *Phys. Rev.* B **4** 3639
[34] Raffaelle R, Anderson H U, Sparlin D M and Parris P E 1991 *Phys. Rev.* B **43** 7991
[35] Philips J C 1989 *Physics of High-T_c Superconductors* (San Diego, CA: Academic) ch 4
[36] Koffyberg F P and Benko F A 1980 *J. Non-Cryst. Solids* **40** 7
[37] Jonker G H 1954 *Physica* **20** 1118
[38] Argall F and Jonscher A K 1968 *Thin Solid Films* **2** 185
[39] Rockstad H K 1970 *J. Non-Cryst. Solids* **2** 192
[40] Owen A E and Robertson J M 1970 *J. Non-Cryst. Solids* **2** 40
[41] Davis E A and Shaw R F 1970 *J. Non-Cryst. Solids* **2** 406
[42] Linsley G S, Owen A E and Hayatee F N 1970 *J. Non-Cryst. Solids* **4** 208
[43] Sayer M, Mansingh A, Reyes J M and Rosenblatt G 1971 *J. Appl. Phys.* **42** 2857
[44] Pike G E 1972 *Phys. Rev.* B **6** 1572
[45] Mott N F 1968 *Phil. Mag.* **17** 1259
[46] Pollak M and Pike G E 1972 *Phys. Rev. Lett.* **28** 1449
[47] Hench L L and West J K 1990 *Principles of Electronic Ceramics* (New York: Wiley) p 205